

Raman analysis of Si/Ge strained-layer superlattices under hydrostatic pressure

Cite as: Appl. Phys. Lett. **58**, 2351 (1991); <https://doi.org/10.1063/1.104894>

Submitted: 17 December 1990 • Accepted: 28 February 1991 • Published Online: 04 June 1998

Zhifeng Sui, Irving P. Herman and Joze Bevk



View Online



Export Citation

ARTICLES YOU MAY BE INTERESTED IN

[Phonon strain shift coefficients in \$\text{Si}_{1-x}\text{Ge}_x\$ alloys](#)

Journal of Applied Physics **103**, 093521 (2008); <https://doi.org/10.1063/1.2913052>

[Band structure, deformation potentials, and carrier mobility in strained Si, Ge, and SiGe alloys](#)

Journal of Applied Physics **80**, 2234 (1996); <https://doi.org/10.1063/1.363052>

 QBLOX



1 qubit

Shorten Setup Time
Auto-Calibration
More Qubits

Fully-integrated
Quantum Control Stacks
Ultrastable DC to 18.5 GHz
Synchronized <<1 ns
Ultralow noise



100s qubits

[visit our website >](#)

Raman analysis of Si/Ge strained-layer superlattices under hydrostatic pressure

Zhifeng Sui and Irving P. Herman

*Department of Applied Physics and the Microelectronics Sciences Laboratories, Columbia University,
New York, New York 10027*

Joze Bevk

AT&T Bell Laboratories, Murray Hill, New Jersey 07974

(Received 17 December 1990; accepted for publication 28 February 1991)

Raman scattering was used to study optical phonons in a $\text{Si}_{12}\text{Ge}_4$ strained-layer superlattice on $c\text{-Si}(001)$ that was subjected to hydrostatic pressure at room temperature. The change of phonon frequency with pressure, $d\omega/dP$, for the principal quasi-confined LO mode in the Ge layers, is found to be significantly smaller than that for bulk crystalline Ge. This difference is shown to be due to the tuning of biaxial strain in the Ge layers and the pressure response of the confined mode as hydrostatic pressure is varied. Both strain and confinement make comparable contributions to $d\omega/dP$ for the Ge layers in the superlattice examined here.

Ultrathin Si/Ge strained layer superlattices (SLSs) have been grown recently with high quality crystallinity, by using molecular beam epitaxy (MBE), despite the significant lattice mismatch ($\sim 4\%$) between Si and Ge.^{1,2} The electronic properties of Si/Ge superlattices are of particular interest because of the possibility of obtaining quasi-direct-gap behavior through a combination of zone folding and strain effects.³⁻⁸ Raman studies of the structural properties of Si/Ge superlattices have yielded useful information on strain, confinement, and interfacial disorder.⁹⁻¹¹ Of particular importance is the effect of strain, which can shift and split both the conduction band and valence band, and thereby change the band offsets.¹² The application of high pressure provides a new method to study the effects of strain and confinement in layered structures. When hydrostatic pressure is applied to a SLS, the lattice mismatch between alternating layers changes because of the different compressibilities of the two materials in these layers. Consequently, in commensurately grown structures, biaxial strain can be tuned by varying the applied hydrostatic pressure. Moreover, the shift of each confined mode frequency with applied pressure differs from that of the zone-center longitudinal optical (LO) phonon because the Grüneisen parameter varies across the LO phonon dispersion curve. We present a Raman study of the strains in SLSs by subjecting a Si/Ge superlattice to high pressure in a diamond anvil cell (DAC), and then analyzing it by Raman spectroscopy. The change in phonon frequency of the strained Ge layer with pressure is shown to be lower than that of bulk $c\text{-Ge}$, and this is attributed to the change of strain and the effect of confinement in these pseudomorphic layers with applied pressure. This is apparently the first Raman study of a SLS subjected to hydrostatic pressure.

The superlattice was grown by MBE on top of a 2700 Å Si buffer layer which had been grown on a Si(001) substrate. The growth temperature was 375–400 °C. The basic unit of the superlattice sample consists of 12 monolayers of Si followed by 4 monolayers of Ge ($\text{Si}_{12}\text{Ge}_4$), and is repeated 25 times. A 140 Å Si cap layer was grown to

protect the superlattice. The SLS substrate was mechanically thinned to 50 μm , and then loaded along with ruby chips and a 4:1 methanol-ethanol fluid mixture into a gasketed Mao-Bell diamond anvil cell in order to apply hydrostatic pressure. The pressure (P) in the DAC was determined by using the calibration scale for ruby R_1 fluorescence versus pressure. Raman spectra of the Si/Ge SLS were taken at room temperature using the 4880 Å line from a cw argon ion laser in the backscattering configuration, with dispersion by a triple grating spectrometer and detection by an intensified diode array. It was necessary to subtract the background diamond fluorescence from these spectra.

The Raman spectrum of this Si/Ge SLS is characterized by the presence of three main peaks, assigned in order of increasing energy to Ge, Ge-Si-like, and Si vibrations. Two representative Raman spectra are shown in Fig. 1, corresponding to ambient pressure (1 bar) and 62.5 kbar, the maximum applied pressure in the experiment. As applied pressure is increased within this range, the biaxial strain in the Ge layers decreases from $\sim 4.0\%$ to $\sim 3.3\%$. Only one Ge peak was found, at 308.0 cm^{-1} for $P = 1$ bar; it was asymmetric with a tail towards lower energy. This peak corresponds to the principal quasi-confined mode in the Ge layers, and is shifted in energy with respect to that in bulk $c\text{-Ge}$ (301.3 cm^{-1} at $P = 1$ bar). The big Si peak near 520 cm^{-1} is from the unstrained $c\text{-Si}$ contributed by the cap layer, superlattice Si layers, the buffer layer, and the substrate.

The Raman shifts of each feature versus pressure are shown in Fig. 2. Least-square straight lines are also plotted for these data, yielding $d\omega/dP$ values for each peak. $d\omega/dP$ is 0.31 ± 0.03 , 0.45 ± 0.03 , and $0.47 \pm 0.02\text{ cm}^{-1}/\text{kbar}$ for the Ge, Ge-Si-like, and Si peaks, respectively. For comparison, the Raman shifts versus pressure for bulk $c\text{-Ge}$ and $c\text{-Si}$ were also measured in this same pressure range, giving 0.37 ± 0.02 and $0.49 \pm 0.02\text{ cm}^{-1}/\text{kbar}$ for $c\text{-Ge}$ and $c\text{-Si}$, respectively. $d\omega/dP$ for the Ge phonon in the SLS is $0.06\text{ cm}^{-1}/\text{kbar}$ smaller than that in $c\text{-Ge}$.

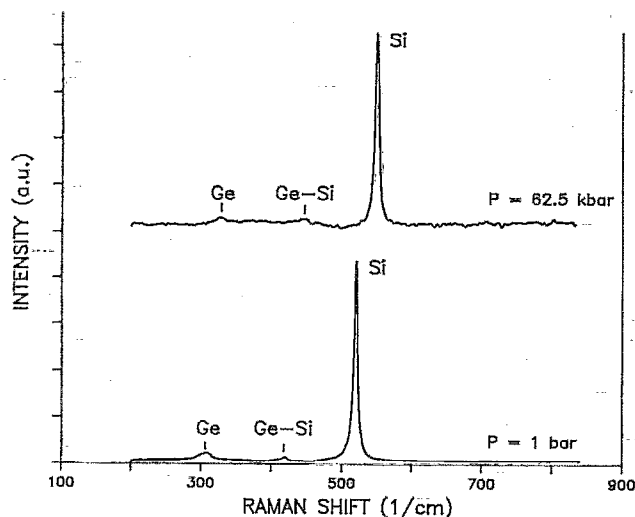


FIG. 1. Raman spectra taken at $P = 1$ bar and $P = 62.5$ kbar are shown ($T = 295$ K). The peaks in order of increasing energy are the principal quasi-confined Ge mode, Ge-Si-like mode and Si mode.

Lattice dynamics and linear chain model calculations of Si/Ge SLSs^{10,13} show that there are confined modes in thin Si layers, and quasi-confined modes in thin Ge layers, even though the Ge optic and Si acoustic modes overlap in energy. In most Raman studies of Si/Ge SLSs only the principal quasi-confined Ge mode is observed. The higher-order modes are usually weak and sensitive to the interfacial ordering.^{11,14,15} At ambient pressure, the frequency of the principal confined Ge optic phonon in the SLS examined here is 6.7 cm^{-1} higher than that in *c*-Ge. The compressive stress in the Ge layer is expected to increase ω by 15.8 cm^{-1} , suggesting that the quasi-confinement decreases ω by $\sim 9 \text{ cm}^{-1}$. This conclusion agrees with other experimental results and with an estimate from the LO phonon dispersion curve.^{9,11} Both theory and experiment^{10,11} agree that the confinement shift for the principal Si optic mode is rather small ($< 2 \text{ cm}^{-1}$) for the 12 monolayer Si layers in this SLS. The strain-induced shift in these Si layers is virtually zero since the SLS is pseudomorphically grown on a Si substrate. Therefore, the confined pho-

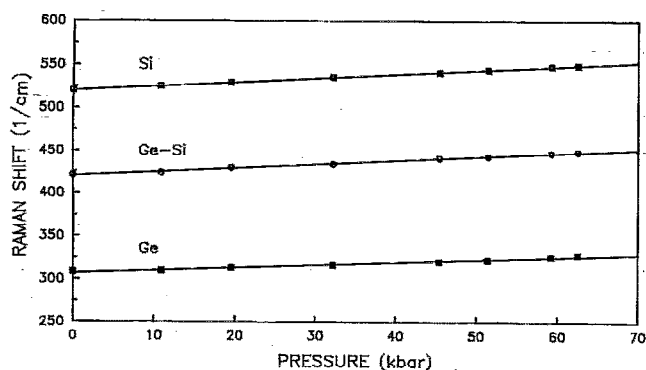


FIG. 2. Plot of the Raman shifts as a function of hydrostatic pressure for three peaks. Least-square fits yield $d\omega/dP = 0.31 \pm 0.03$, 0.45 ± 0.02 , and $0.47 \pm 0.02 \text{ cm}^{-1}/\text{kbar}$ for the Ge, Ge-Si-like, and Si peaks, respectively.

non feature in the Si SLS layers is expected to overlap the *c*-Si peak, as is seen here.

From the analysis of Cerdeira *et al.*,¹⁶ it follows that when a strain is applied along the major crystal axes, the dynamical equation in the [001] direction is decoupled from the other two directions. Therefore, the Raman frequency for an optical phonon in Ge layers of the SLS along the [001] direction, in the absence of confinement and interfacial disorder, is

$$\omega = \omega_0 + (1/2\omega_0)[p\epsilon_{zz} + q(\epsilon_{xx} + \epsilon_{yy})], \quad (1)$$

where the ω_0 is the frequency of the *c*-Ge zone-center LO phonon, p and q are the Ge deformation potentials defined in Ref. 6, and ϵ_{ii} are the diagonal elements of the strain tensor. In the presence of hydrostatic pressure and biaxial stress, ϵ_{ii} can be decomposed into $\epsilon_{ii} = \epsilon_{ii}^{(h)} + \epsilon_{ii}^{(b)}$. $\epsilon_{ii}^{(h)}$ is the hydrostatic strain, which has the form

$$\epsilon_{xx}^{(h)} = \epsilon_{yy}^{(h)} = \epsilon_{zz}^{(h)} = -P/(C_{11}^{\text{Ge}} + 2C_{12}^{\text{Ge}}), \quad (2)$$

where C_{11}^{Ge} and C_{12}^{Ge} are the elastic constants for Ge, and P is the applied hydrostatic pressure. The biaxial strain in the Ge layers is

$$\epsilon_{xx}^{(b)} = \epsilon_{yy}^{(b)} = [a^{\text{Si}}(P) - a^{\text{Ge}}(P)]/a^{\text{Ge}}(P), \quad (3)$$

where $a(P)$ is the lattice constant at pressure P ; also

$$\epsilon_{zz}^{(b)} = -(2C_{12}^{\text{Ge}}/C_{11}^{\text{Ge}})\epsilon_{xx}^{(b)}. \quad (4)$$

Inserting Eqs. (2)–(4) into Eq. (1) gives

$$\omega = \omega_0 + \frac{1}{\omega_0} \left(q - p \frac{C_{12}^{\text{Ge}}}{C_{11}^{\text{Ge}}} \right) \left(\frac{a_0^{\text{Si}}}{a_0^{\text{Ge}}} - 1 \right) - \frac{p + 2q}{2\omega_0(C_{11}^{\text{Ge}} + 2C_{12}^{\text{Ge}})} P + \frac{1}{\omega_0} \frac{a_0^{\text{Si}}}{a_0^{\text{Ge}}} \left(q - p \frac{C_{12}^{\text{Ge}}}{C_{11}^{\text{Ge}}} \right) \left[\frac{1}{C_{11}^{\text{Ge}} + 2C_{12}^{\text{Ge}}} - \frac{1}{C_{11}^{\text{Si}} + 2C_{12}^{\text{Si}}} \right] P, \quad (5)$$

where a_0 is the lattice constant at ambient pressure. The second term on the right-hand side is the usual lattice mismatch correction due to the compressive strain in Ge layers at ambient pressure, which gives the $+15.8 \text{ cm}^{-1}$ contribution mentioned earlier. The third term is due to hydrostatic pressure applied to bulk Ge. The fourth term is due to the change in Ge and Si lattice constants with pressure because Ge and Si have different compressibilities; this results in a decrease in compressive strain in Ge layers with increasing pressure.

Inclusion of confinement can modify Eq. (5) in two ways. (1) At ambient pressure, the confined Ge modes for an n -atom layer are not at the zone center frequency ω_0 , but at frequencies $\omega_c^{(m)}$, which are obtained approximately by zone folding the bulk LO dispersion curve at $k^{(m)} = m\pi/nd_0$,¹¹ where d_0 is the monolayer spacing and $m = 1, 2, \dots, n$. This assumes no coupling between confinement and strain, and perfect interfaces. The $m = 1$ mode corresponds to the principal confined mode, which is at $0.5(2\pi/a)$ for the Ge layers of the SLS, where $a = 4d_0$ is the lattice constant. Consequently, ω_0 should be replaced by $\omega_c^{(1)}(k = \pi/a)$. (2) Since the Grüneisen parameter γ varies across the bulk LO phonon dispersion curve, the

TABLE I. Parameters for bulk *c*-Si and *c*-Ge at room temperature.

	Si	Ge
C_{11} (kbar)	1656 ^a	1288 ^a
C_{12} (kbar)	638.6 ^a	482.5 ^a
a_0 (Å)	5.431 ^a	5.646 ^a
ω_0 (s ⁻¹)	0.9849×10^{14} ^b	0.5648×10^{14} ^b
p (s ⁻²)	-1.345×10^{28} ^b	-4.7×10^{27} ^b
q (s ⁻²)	-1.946×10^{28} ^b	-6.167×10^{27} ^b

^aS. S. Mitra and N. E. Massa, in *Handbook on Semiconductors*, edited by T. S. Moss (North Holland, Amsterdam, 1986) Vol. 1, p. 96.

^bReference 16.

pressure-dependent “bulk” contribution, which is the third term on the right-hand side in Eq. (5), will be different for each confined mode. Calculations¹⁷ suggest that γ for LO phonons decreases by ~ 0.044 as k increases from 0 to π/a along (001) in Ge; though this has not been verified experimentally, this value will be assumed here. Since the principal confined mode in the Ge layers is at π/a , the difference in $d\omega/dP$ between $k=\pi/a$ and $k=0$ is estimated to be

$$\left. \frac{d\omega}{dP} \right|_{k=\pi/a} - \left. \frac{d\omega}{dP} \right|_{k=0} = \frac{3(\gamma\Delta\omega_0 + \omega_0\Delta\gamma)}{(C_{11}^{\text{Ge}} + 2C_{12}^{\text{Ge}})} = -0.028 \text{ cm}^{-1}/\text{kbar}, \quad (6)$$

where $\Delta\omega_0 = \omega_c^{(1)} - \omega_0 = -9.0 \text{ cm}^{-1}$. With $\gamma = -(p + 2q)/6\omega_0^2$, p and q at $k=\pi/a$ can be obtained assuming either that p , q , and γ change proportionately from $k=0$ to π/a or that $(p - q)/2\omega_0^2 = 0.23$, for *c*-Ge.¹⁶ In either case, it is seen that the effect of confinement on the fourth term in Eq. (5) is negligible.

Using the parameters listed in Table I for Si and Ge, $d\omega/dP$ for principal confined Ge mode in the Si/Ge SLS, and the zone center optic phonons in *c*-Ge and *c*-Si are expected to be 0.314, 0.355, and 0.481 $\text{cm}^{-1}/\text{kbar}$, respectively, excluding confinement effects. The effect of strain in the Ge layers is expected to decrease $d\omega/dP$ by 0.041 $\text{cm}^{-1}/\text{kbar}$ relative to *c*-Ge. Inclusion of the confinement term decreases the expected value of $d\omega/dP$ in the Ge layers of the SLS to 0.286 $\text{cm}^{-1}/\text{kbar}$, which is 0.069 $\text{cm}^{-1}/\text{kbar}$ lower than the *c*-Ge value. Our corresponding experimental values are 0.31 ± 0.03 , 0.37 ± 0.02 , and $0.49 \pm 0.02 \text{ cm}^{-1}/\text{kbar}$ for the SLS Ge, *c*-Ge, and *c*-Si. This experiment shows that the effects of strain and confinement decrease $d\omega/dP$ in the Ge layers by 0.06 $\text{cm}^{-1}/\text{kbar}$ relative to that in *c*-Ge, which is within experimental error of the prediction. Our measured $d\omega/dP$ values for *c*-Si and *c*-Ge are in agreement with the values obtained

using p and q , and with previously measured values $0.52 \pm 0.03 \text{ cm}^{-1}/\text{kbar}$ for *c*-Si¹⁸ and $0.385 \pm 0.005 \text{ cm}^{-1}/\text{kbar}$ for *c*-Ge,¹⁹ which included a P^2 term in analyzing $\omega(P)$. Including this quadratic term in our analysis brings our $d\omega/dP$ values even closer to those in Refs. 18 and 19.

In conclusion, the difference between $d\omega/dP$ for the principal quasi-confined LO mode in Ge layers in a Si/Ge SLS and that in bulk *c*-Ge can be explained by biaxial strain and confinement. The perturbation on $d\omega/dP$ for Ge due to confinement is comparable in magnitude and has the same sign as that due to strain. In contrast, confinement and strain lead to perturbations of roughly comparable magnitudes but opposite signs in the Raman frequency measurement at ambient pressure. With improved precision, the Grüneisen parameter for Si and Ge LO phonons from the Γ to the X point can be determined from Raman measurements of $d\omega/dP$ in Si_nGe_m SLSs on (001) substrates for different n and m , and that for several other optical branches can be obtained using SLSs grown on substrates with different crystal orientations.

This work was supported at Columbia by the Joint Services Electronics Program Contract DAAL 03-88-C-0009 and by the Office of Naval Research. The authors would like to thank Judah A. Tuchman for his valuable advice and assistance regarding diamond anvil cell technique.

- ¹J. Bevk, A. Ourmazd, L. C. Feldman, T. P. Pearsall, J. M. Bonar, B. A. Davidson, and J. P. Mannaerts, *Appl. Phys. Lett.* **50**, 760 (1987).
- ²E. Kasper, H. Kibbel, H. Jorke, H. Brugger, E. Friess, and G. Abstreiter, *Phys. Rev. B* **38**, 3599 (1988).
- ³R. People and S. A. Jackson, *Phys. Rev. B* **36**, 1310 (1987).
- ⁴M. S. Hybertsen and M. Schlüter, *Phys. Rev. B* **36**, 9683 (1987).
- ⁵S. Froyen, D. M. Wood, and A. Zunger, *Phys. Rev. B* **36**, 4547 (1987); *Appl. Phys. Lett.* **54**, 2435 (1989).
- ⁶S. Satpathy, R. M. Martin, and C. G. Van de Walle, *Phys. Rev. B* **38**, 13237 (1988).
- ⁷M. A. Gell, *Phys. Rev. B* **38**, 7535 (1988).
- ⁸T. P. Pearsall, *Crit. Rev. Solid State Mater. Sci.* **15**, 551 (1989), and references cited therein.
- ⁹J. Menendez, A. Pinczuk, J. Bevk, and J. P. Mannaerts, *J. Vac. Sci. Technol. B* **6**, 1306 (1988).
- ¹⁰M. W. C. Dharma-Wardana, G. C. Aers, D. J. Lockwood, and J.-M. Baribeau, *Phys. Rev. B* **41**, 5319 (1990).
- ¹¹E. Friess, K. Eberl, U. Menzinger, and G. Abstreiter, *Solid State Commun.* **73**, 203 (1990).
- ¹²G. P. Schwartz, M. S. Hybertsen, J. Bevk, R. G. Nuzzo, J. P. Mannaerts, and G. J. Gualtieri, *Phys. Rev. B* **39**, 1235 (1989).
- ¹³A. Fasolino and E. Molinari, *J. De Physique (Paris)* **48**, C5-569 (1987).
- ¹⁴S. Wilke, *Solid State Commun.* **73**, 399 (1990).
- ¹⁵S. Wilke, J. Mašek, and B. Velický, *Phys. Rev. B* **41**, 3769 (1990).
- ¹⁶F. Cerdeira, C. J. Buchenauer, F. H. Pollak, and M. Cardona, *Phys. Rev. B* **5**, 580 (1972).
- ¹⁷G. Dolling and R. A. Cowley, *Proc. Phys. Soc. London* **88**, 463 (1966).
- ¹⁸B. A. Weinstein and G. J. Piermarini, *Phys. Rev. B* **12**, 1172 (1975).
- ¹⁹D. Olego and M. Cardona, *Phys. Rev. B* **25**, 1151 (1982).